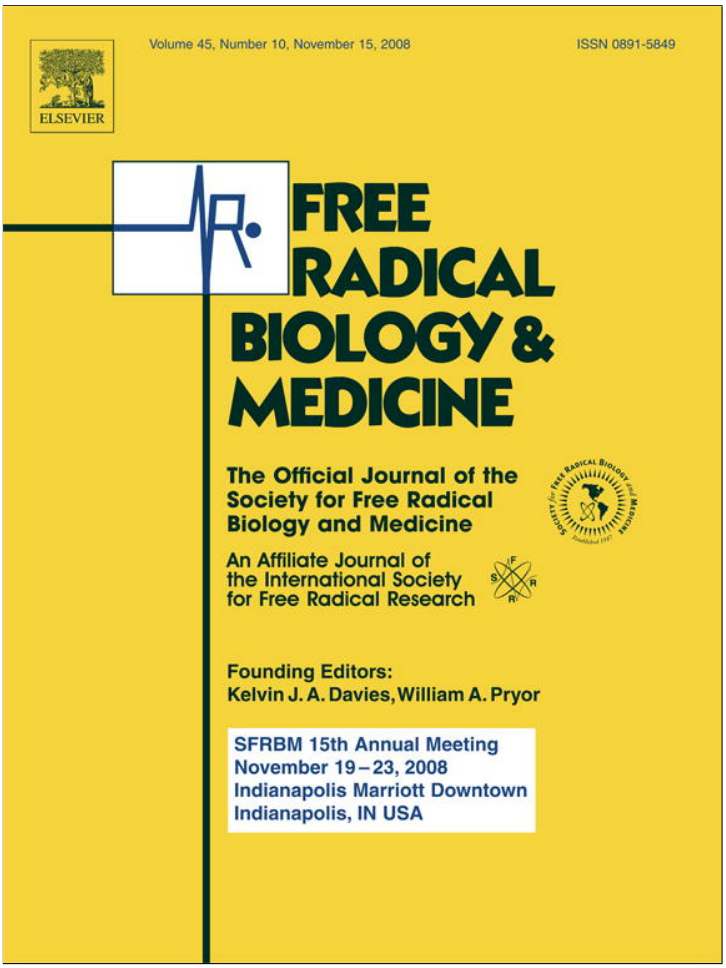

Free Radical Biology & Medicine 45 (2008) 1395–1402

Contents lists available at ScienceDirect

Free Radical Biology & Medicine

journal homepage: www.elsevier.com/locate/freeradbiomed

Original Contribution

Doxorubicin increases the susceptibility of brain mitochondria to Ca^{2+}-induced permeability transition and oxidative damage

Susana Cardoso [a,1], Renato X. Santos [a,1], Cristina Carvalho [a,1], Sónia Correia [a,b,1], Gonçalo C. Pereira [a,b], Susana S. Pereira [a,b], Paulo J. Oliveira [a,b], Maria S. Santos [a,b], Teresa Proença [b,c], Paula I. Moreira [b,d,*]

[a] Department of Zoology, Faculty of Sciences and Technology, University of Coimbra, 3000-354 Coimbra, Portugal
[b] Center for Neuroscience and Cell Biology, University of Coimbra, 3004-517 Coimbra, Portugal
[c] Department of Neurology, Coimbra University Hospital, University of Coimbra, 3000-354 Coimbra, Portugal
[d] Institute of Physiology, Faculty of Medicine, University of Coimbra, 3000-354 Coimbra, Portugal

ARTICLE INFO

Article history:
Received 18 June 2008
Revised 3 August 2008
Accepted 5 August 2008
Available online 14 August 2008

Keywords:
Brain
Doxorubicin
Mitochondria
Oxidative stress
Permeability transition pore
Free radicals

ABSTRACT

This study was aimed at investigating the effects of subchronic administration of doxorubicin (DOX) on brain mitochondrial bioenergetics and oxidative status. Rats were treated with seven weekly injections of vehicle (sc, saline solution) or DOX (sc, 2 mg kg^{-1}), and 1 week after the last administration of the drug the animals were sacrificed and brain mitochondrial fractions were obtained. Several parameters were analyzed: respiratory chain, phosphorylation system, induction of the permeability transition pore (PTP), mitochondrial aconitase activity, lipid peroxidation markers, and nonenzymatic antioxidant defenses. DOX treatment induced an increase in thiobarbituric acid-reactive substances and vitamin E levels and a decrease in reduced glutathione content and aconitase activity. Furthermore, DOX potentiated PTP induced by Ca^{2+}. No statistical differences were observed in the other parameters analyzed. Altogether our results show that DOX treatment increases the susceptibility of brain mitochondria to Ca^{2+}-induced PTP opening and oxidative stress, predisposing brain cells to degeneration and death.

Introduction

Doxorubicin (DOX) is a potent broad-spectrum antineoplastic agent effective in the treatment of a wide variety of cancers, including both solid tumors and leukemias [1]. However, the chronic administration of this drug can induce toxicity to nontarget tissues, cardiotoxicity being the best known side effect [2]. DOX-induced cardiotoxicity has been attributed to a number of effects, including the direct inhibition of key transporters involved in ion homeostasis, alterations in cellular iron and calcium metabolism, disruption of sarcoplasmic reticulum function, mitochondrial dysfunction, and apoptotic cell loss [3]. The mechanisms underlying these events seem to be linked to an increased production of reactive oxygen species (ROS) and oxidative damage [3]. Oxidative stress results from an imbalance between the generation of ROS and reactive nitrogen species and their removal by the cellular antioxidant system [4] and has been implicated in many neurodegenerative disorders [5,6].

Several studies in breast cancer survivors and other patients undergoing DOX-based chemotherapy have reported persistent changes in cognitive functions, including memory loss and difficulty in the performance of daily life tasks [4]. Despite the well-known side effects of DOX treatment in the heart, little is known about its effects in the brain. Park et al. [7] showed that DOX generates free radicals in cultured astrocytes and decreases cell viability in a concentration-dependent manner. Similarly, in a study made in primary neuronal cultures, Lopes et al. [2] observed that DOX can induce neuronal cell death by necrosis and apoptosis in a concentration-dependent manner.

Mitochondria play a central role in both cell life and cell death [8]. These organelles are essential for the production of ATP through oxidative phosphorylation and regulation of intracellular Ca^{2+} homeostasis and are the main generators of intracellular ROS. Furthermore, mitochondria play a key role in controlling pathways that lead to apoptosis. Defects of mitochondrial function can result in the excessive production of ROS, formation of the permeability transition pore (PTP), and release of apoptotic proteins. Therefore, several mitochondrial structures and mechanisms provide primary targets for drug-induced toxicity and cell death [9]. Indeed, it has been reported that mitochondria are the main targets of DOX-induced cardiac toxicity [10–13].

In light of these results, the aim of this study was to evaluate the effect of DOX treatment on brain mitochondrial function and oxidative status. Our hypothesis is that in vivo DOX administration to Wistar rats results not only in decreased mitochondrial function but also in increased susceptibility to Ca^{2+}-induced PTP and oxidative damage. To

* Corresponding author. Center for Neuroscience and Cell Biology, University of Coimbra, 3004-517 Coimbra, Portugal.
E-mail addresses: venta@ci.uc.pt, pismoreira@gmail.com (P.I. Moreira).
[1] These authors contributed equally to this work.

0891-5849/$ – see front matter © 2008 Elsevier Inc. All rights reserved.
doi:10.1016/j.freeradbiomed.2008.08.008

test our hypothesis we evaluated several parameters from the respiratory chain function [States 2, 3, and 4 of mitochondrial respiration, respiratory control ratio (RCR), ADP/O index, carbonylcyanide *p*-trifluoromethoxyphenyl-hydrazone (FCCP)-stimulated respiration, oligomycin-inhibited respiration], phosphorylation system [mitochondrial transmembrane potential ($\Delta\Psi_m$), repolarization level, repolarization lag phase, and ATP levels], Ca^{2+}-induced PTP ($\Delta\Psi_m$, Ca^{2+}fluxes, and protein thiol group oxidation), mitochondrial aconitase activity, lipid peroxidation markers [thiobarbituric acid-reactive substances (TBARS) and malondialdehyde (MDA)], and levels of nonenzymatic antioxidant defenses [vitamin E and reduced (GSH) and oxidized (GSSG) glutathione].

Materials and methods

Materials

Doxorubicin was obtained from Sigma (Portugal). All the other chemicals were of the highest grade of purity commercially available.

Animals

Male Wistar rats (16 weeks of age) were housed in our animal colony (Laboratory Research Center, Faculty of Medicine, University of Coimbra). Rats were kept under controlled light (12-h day/night cycle) and humidity with free access (except in the fasting period) to water and powdered rodent chow (URF1; Charles River). Rats were treated with seven weekly injections of vehicle (sc, saline solution, NaCl 0.9%) or DOX (sc, 2 mg kg^{-1}). In adherence to procedures approved by the Institutional Animal Care and Use Committee, the animals were sacrificed by cervical displacement and decapitation 1 week after the last administration of DOX.

Mitochondrial fraction isolation

For the PTP studies, brain mitochondria were isolated from rats by the method of Rosenthal et al. [14], with slight modifications, using 0.02% digitonin to free mitochondria from the synaptosomal fraction. In brief, the rat was decapitated, and the whole brain minus the cerebellum was rapidly removed, washed, minced, and homogenized at 4°C in 10 ml of isolation medium (225 mM mannitol, 75 mM sucrose, 5 mM Hepes, 1 mM EGTA, 1 mg/ml bovine serum albumin (BSA), pH 7.4) containing 5 mg of bacterial protease type VIII (subtilisin). Single brain homogenates were brought to 30 ml and then centrifuged at 2500 rpm (Sorvall RC-5B refrigerated superspeed centrifuge) for 5 min. The pellet, including the fluffy synaptosomal layer, was resuspended in 10 ml of the isolation medium containing 0.02% digitonin and centrifuged at 10,000 rpm for 10 min. The brown mitochondrial pellet without the synaptosomal layer was then resuspended again in 10 ml of medium and centrifuged at 10,000 rpm for 5 min. The pellet was resuspended in 10 ml of washing medium (225 mM mannitol, 75 mM sucrose, 5 mM Hepes, pH 7.4) and centrifuged at 10,000 rpm for 5 min. The final mitochondrial pellet was resuspended in 150 μl of the washing medium.

Other experiments were performed with crude brain mitochondrial fractions. Briefly, after animal decapitation, whole cerebral cortices were rapidly removed and homogenized in 10 ml of homogenization medium (0.32 M sucrose, 10 mM Hepes, and 0.5 mM EGTA–K^+, pH 7.4). The homogenate was centrifuged at 2500 rpm for 10 min and the supernatant was again centrifuged at 10,000 rpm for 10 min. The pellet was resuspended in 10 ml of washing medium (0.32 M sucrose, 10 mM Hepes, pH 7.4) and centrifuged at 10,000 rpm for 10 min. For the final pellet the white and fluffy synaptosome layer was removed and the brown mitochondrial layer was resuspended in 200 μl of washing medium. Mitochondrial protein was determined by the biuret method calibrated with BSA [15].

Mitochondrial respiration measurements

Oxygen consumption by the brain mitochondria was registered polarographically with a Clark oxygen electrode [16] connected to a suitable recorder in a thermostated water-jacketed closed chamber with magnetic stirring. The reactions were carried out at 30°C in 1 ml of the standard medium (100 mM sucrose, 100 mM KCl, 2 mM KH_2PO_4, 5 mM Hepes, and 10 μM EGTA, pH 7.4) with 0.8 mg of protein. State 2 of mitochondrial respiration was initiated with 5 mM glutamate/2.5 mM malate (mitochondrial energization through complex I) or 5 mM succinate in the presence of 2 μM rotenone (mitochondrial energization through complex II). The RCR is the ratio between State 3 (consumption of oxygen in the presence of substrate and 155 nmol ADP/mg protein) and State 4 (consumption of oxygen after ADP has been consumed) of mitochondrial respiration. The ADP/O index is expressed by the ratio between the amount of ADP added and the oxygen consumed during State 3 of mitochondrial respiration. FCCP-stimulated respiration was induced with the addition of 1 μM FCCP and oligomycin-inhibited respiration was achieved with the addition of 200 μg oligomycin per milliliter.

Mitochondrial membrane potential measurements

$\Delta\Psi_m$ was monitored by evaluating the transmembrane distribution of the lipophilic cation tetraphenylphosphonium (TPP^+) with a TPP^+-selective electrode prepared according to Kamo et al. [17] using an Ag/AgCl-saturated electrode (Tacussel, Model MI 402) as reference. TPP^+uptake has been measured from the decreased TPP^+concentration in the medium sensed by the electrode. The potential difference between the selective electrode and the reference electrode was measured with an electrometer and recorded continuously in a Linear 1200 recorder. The voltage response of the TPP^+electrode to log[TPP^+] was linear with a slope of 59 ± 1, in good agreement with the Nernst equation. Reactions were carried out in a chamber with magnetic stirring in 1 ml of the standard medium containing 3 μM TPP^+. This TPP^+concentration was chosen to achieve high sensitivity in measurements and to avoid possible toxic effects on mitochondria [18]. The $\Delta\Psi_m$ was estimated by the equation $\Delta\Psi_m$ (mV)= 59 log(v/V) − 59 log($10^{\Delta E/59}$ − 1) as indicated by Kamo et al. [17] and Muratsugu et al. [19]. *v*, *V*, and Δ*E* stand for mitochondrial volume, volume of the incubation medium, and deflection of the electrode potential from the baseline, respectively. This equation was derived assuming that the TPP^+distribution between the mitochondria and the medium follows the Nernst equation and that the law of mass conservation is applicable. A matrix volume of 1.1 μl/mg protein was assumed. No correction was made for the "passive'' binding contribution of TPP^+ to the mitochondrial membranes, because the purpose of the experiments was to show relative changes in potentials rather than absolute values. As a consequence, we can anticipate a slight overestimation on $\Delta\Psi_m$ values. However, the overestimation is significant only at $\Delta\Psi_m$ values below 90 mV and, therefore, far from our measurements. Mitochondria (0.8 mg/ml) were energized with 5 mM glutamate/2.5 mM malate or 5 mM succinate in the presence of 2 μM rotenone. After a steady-state distribution of TPP^+ had been reached (ca. 1 min of recording), $\Delta\Psi_m$ fluctuations were recorded. For the PTP experiments, two or three pulses of Ca^{2+}(first pulse, 25 nmol Ca^{2+}; second and third pulses, 20 nmol Ca^{2+}) were added, and $\Delta\Psi_m$ was recorded. Cyclosporin A (CsA; 0.85 μM) and 2 μg/ml oligomycin plus 1 mM ADP were added 2 min before Ca^{2+}addition.

Determination of adenine nucleotide levels

At the end of each $\Delta\Psi_m$ measurement, 250 μl of each sample was promptly centrifuged at 14,000 rpm (Eppendorf centrifuge 5415C) for 2 min with 250 μl of 0.3 M perchloric acid ($HClO_4$). The supernatants were neutralized with 10 M KOH in 5 M Tris and again centrifuged at 14,000 rpm for 2 min. The resulting supernatants

were assayed for adenine nucleotide by separation by reverse-phase high-performance liquid chromatography (HPLC). The HPLC apparatus was a Beckman-System Gold, consisting of a 126 binary pump model and 166 variable UV detector controlled by a computer. The detection wavelength was 254 nm, and the column was a Lichrospher 100 RP-18 (5 μm) from Merck. An isocratic elution with 100 mM phosphate buffer (KH_2PO_4; pH 6.5) and 1.2% methanol was performed with a flow rate of 1 ml/min. The required time for each analysis was 5 min. Adenine nucleotides were identified by their chromatographic behavior (retention time, absorption spectra, and correlation with standards).

Measurement of Ca^{2+}fluxes

Mitochondrial Ca^{2+}fluxes were measured by monitoring the changes in Ca^{2+}concentration in the reaction medium using the hexapotassium salt of the fluorescence probe Calcium Green 5-N [20]. Mitochondria (0.8 mg) were resuspended in 2 ml of reaction medium supplemented with 100 nM Calcium Green 5-N followed by addition of Ca^{2+}(45 nmol) and energization with 5 mM succinate. Fluorescence was continuously recorded in a water-jacketed cuvette holder at 30°C using a Perkin–Elmer spectrofluorometer LS-50 B with excitation wavelength of 506 nm (slit 4 nm) and emission wavelength of 532 nm (slit 6 nm).

Measurement of mitochondrial thiol oxidation

A variation of Ellman's method was used to determine the mitochondrial content in protein thiol groups [21]. At the end of the ΔΨm experiments concerning PTP evaluation (in the presence/absence of Ca^{2+}), 750 μl of each mitochondrial suspension was frozen and thawed three times. Then, 750 μl of sulfosalicylic acid 4% was added to each sample. The samples were then subjected to centrifugation at 10,000 rpm for 15 min. The supernatant was removed and the pellet was suspended in 1 ml of phosphate buffer 100 mM, pH 8. The suspension was sonicated and diluted to 2.6 ml in phosphate buffer medium containing 385 mM 5,5′-dithiobis(2-nitrobenzoic) acid. After 15 min of reaction, the absorption was measured at 412 nm, and the results were expressed as a percentage of control.

Measurement of thiobarbituric acid-reactive substance levels

TBARS levels were determined by using the thiobarbituric acid assay, according to a modified procedure described by Ernster and Nordenbrand [22]. The amount of TBARS formed was calculated using a molar coefficient of 1.56×10^5 mol^{-1} cm^{-1} and expressed as nmol TBARS/mg protein.

Measurement of malondialdehyde levels

MDA levels were determined by HPLC [23]. Liquid chromatography was performed using a Gilson HPLC apparatus with a reverse-phase column (RP18 Spherisorb, S5 OD2). The samples were eluted from the column at a flow rate of 1 ml/min and detection was performed at 532 nm. The MDA content of the samples was calculated from a standard curve prepared using the thiobarbituric acid–MDA complex and was expressed as nmol/mg protein.

Measurement of reduced and oxidized glutathione contents

GSH and GSSG levels were determined with fluorescence detection after reaction of the supernatants from deproteinized mitochondria containing H_3PO_4/NaH_2PO_4–EDTA or H_3PO_4/NaOH, respectively, with *o*-phthalaldehyde (OPT), pH 8.0, according to Hissin and Hilf [24]. In brief, freshly isolated brain mitochondria (0.5 mg) resuspended in 1.5 ml phosphate buffer (100 mM NaH_2PO_4, 5 mM EDTA, pH 8.0) and 500 μl H_3PO_4 4.5% were rapidly centrifuged at 50,000 rpm (Beckman, TL-100 ultracentrifuge) for 30 min. For GSH determination, 100 μl of supernatant was added to 1.8 ml phosphate buffer and 100 μl OPT. After thorough mixing and incubation at room temperature for 15 min, the solution was transferred to a quartz cuvette and the fluorescence was measured at 420 and 350 nm emission and excitation wavelengths, respectively. For GSSG determination, 250 μl of the supernatant was added to 100 μl of *N*-ethylmaleimide and incubated at room temperature for 30 min. After the incubation, 140 μl of the mixture was added to 1.76 ml NaOH (100 mM) buffer and 100 μl OPT. After mixing and incubation at room temperature for 15 min, the solution was transferred to a quartz cuvette and the fluorescence was measured at 420 and 350 nm emission and excitation wavelengths, respectively. GSH and GSSG contents were determined from comparisons with a linear GSH or GSSG standard curve, respectively.

Measurement of vitamin E content

Extraction and separation of vitamin E (α-tocopherol) from brain mitochondria were performed by following a method previously described by Vatassery and Younoszai [25]. Briefly, 1.5 ml sodium dodecyl sulfate (10 mM) was added to 0.5 mg of freshly isolated brain mitochondria, followed by the addition of 2 ml ethanol. Then 2 ml hexane and 50 μl of 3 M KCl were added, and the mixture was vortexed for about 3 min. The extract was centrifuged at 2000 rpm (Sorvall RT6000 refrigerated centrifuge) and 1 ml of the upper phase, containing *n*-hexane, was recovered and evaporated to dryness under a stream of N_2 and kept at −80°C. The extract was dissolved in *n*-hexane, and vitamin E content was analyzed by reverse-phase high-performance liquid chromatography. A Spherisorb S10w column (4.6 200 nm) was eluted with *n*-hexane modified with 0.9% methanol, at a flow rate of 1.5 ml/min. Detection was performed by a UV detector at 287 nm. The content of mitochondrial vitamin E was calculated as nmol/mg protein.

Measurement of aconitase activity

Aconitase activity was determined according to Krebs and Holzach [26]. Briefly, the brain mitochondrial fraction (200 μg) was diluted in 0.6 ml buffer containing 50 mM Tris–HCl and 0.6 mM $MnCl_2$ (pH 7.4) and sonicated for 10 s. Aconitase activity was immediately measured spectrophotometrically by monitoring at 240 nm the *cis*-aconitase after addition of 20 mM isocitrate at 25°C. The activity of aconitase was calculated using a molar coefficient of 3.6 mM^{-1} cm^{-1} and expressed as U/mg protein/min. One unit was defined as the amount of enzyme necessary to produce 1 μM *cis*-aconitate per minute.

Statistical analysis

Results are presented as means ± SEM of the indicated number of experiments. Statistical significance was determined using the paired Student *t* test and one-way ANOVA for multiple comparisons, followed by the post hoc Tukey–Kramer test.

Results

DOX does not affect the mitochondrial respiration chain nor the phosphorylation system

The mitochondrial transmembrane potential is fundamental for the phenomenon of oxidative phosphorylation, which results in the conversion of ADP to ATP via ATP synthase. The mitochondrial respiratory chain pumps H^+out of the mitochondrial matrix across the inner mitochondrial membrane. The H^+gradient originates an electrochemical potential resulting in a pH and a voltage gradient ($\Delta\Psi_m$)

Table 1
Effect of DOX treatment on States 2, 3, and 4 of mitochondrial respiration

	Glutamate/malate		Succinate	
	Saline	DOX	Saline	DOX
State 2 (nAtgO/min/mg)	17.4±2.24	14.9±2.09	12.1±1.02	11.4±1.08
State 3 (nAtgO/min/mg)	54.4±4.76	48.3±4.09	44.2±4.00	37.7±2.65
State 4 (nAtgO/min/mg)	16.7±0.89	14.8±1.15	23.5±1.81	19.0±0.88

States 2, 3, and 4 of mitochondrial respiration were evaluated in freshly isolated brain mitochondrial fractions (0.8 mg) in 1 ml of the reaction medium energized with 5 mM glutamate/2.5 mM malate or with 5 mM succinate in the presence of 2 μM rotenone. Data shown represent means±SEM of four or five animals from each condition studied. nAtgO/min/mg = nAtom-gram oxygen/min/mg.

Table 2
Effect of DOX treatment on the mitochondrial oxidative phosphorylation system [mitochondrial transmembrane potential (Ψ_m), repolarization level, repolarization lag phase, and ATP levels]

	Glutamate/malate		Succinate	
	Saline	DOX	Saline	DOX
$\Delta\Psi_m$ (−mV)	214.7±15.43	213.2±15.90	185.4±1.28	184.2±1.48
Repolarization level (−mV)	146.9±18.86	137.3±19.24	149.5±1.24	149.2±1.68
Repolarization lag phase (min)	1.8±0.21	1.5±0.12	1.5±0.07	1.4±0.07
ATP levels (nmol/mg protein)	58.0±6.00	48.9±4.16	91.2±8.29	98.1±11.69

The oxidative phosphorylation parameters were evaluated in freshly isolated brain mitochondrial fractions (0.8 mg) in 1 ml of the reaction medium supplemented with 3 μM $TPP^+$and energized with 5 mM glutamate/2.5 M malate or with 5 mM succinate in the presence of 2 μM rotenone. Adenine nucleotide levels were determined by HPLC, as described under Materials and methods. Data are the means±SEM of three to five experiments from each condition studied.

across the inner membrane. Compared with mitochondria isolated from saline-injected animals, DOX treatment induced a slight, although not significant, decrease in States 2, 3, and 4 of mitochondrial respiration (Table 1). Furthermore, DOX treatment did not induce any significant alteration in RCR, ADP/O index, FCCP-stimulated respiration, or oligomycin-inhibited respiration (Fig. 1). Similarly, DOX treatment did not induce any significant alteration in $\Delta\Psi_m$, repolarization level (capacity of the mitochondria to recover $\Delta\Psi_m$ after ADP phosphorylation), repolarization lag phase (time necessary for ADP phosphorylation), or ATP levels compared with mitochondria isolated from saline-injected animals (Table 2).

DOX potentiates Ca^{2+}-induced PTP

The PTP is characterized by an increase in mitochondrial membrane permeability that leads to the loss of $\Delta\Psi_m$, alteration in Ca^{2+}fluxes, mitochondrial swelling, and rupture of the outer mitochondrial membrane [27]. As shown in Fig. 2, trace A, mitochondria isolated from saline-treated animals after energization with succinate developed a $\Delta\Psi_m \approx -196$ mV. The first pulse of Ca^{2+}led to a depolarization followed by incomplete repolarization. However, after the second pulse of $Ca^{2+}$the mitochondria depolarized and failed to repolarize, indicating the induction of PTP (Fig. 2, trace A). Mitochondria from DOX-treated animals energized with succinate developed a $\Delta\Psi_m \approx -185$ mV. These mitochondria in the presence of the same two pulses of Ca^{2+}depolarize more rapidly compared to control mitochondria (Fig. 2, trace B). The addition of the PTP inhibitor oligomycin plus ADP prevented mitochondrial depolarization after three pulses of Ca^{2+} (Fig. 2, traces C and D). Mitochondria can tolerate a determined amount of Ca^{2+}, but ultimately their capacity to accumulate Ca^{2+} is overwhelmed and mitochondria completely depolarize owing to a profound change in the inner membrane permeability. When Ca^{2+}

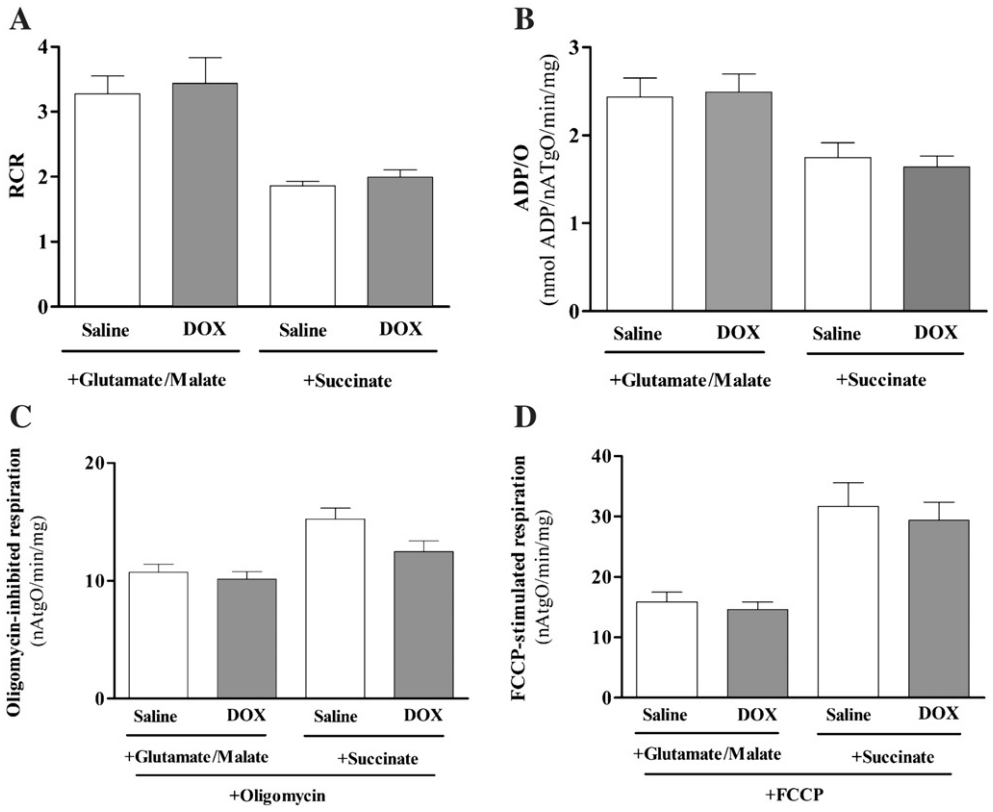

Fig. 1. Effect of DOX treatment on mitochondrial respiratory chain parameters: (A) respiratory control ratio, (B) ADP/O index, (C) oligomycin-inhibited respiration, and (D) FCCP-stimulated respiration. Data shown represent means ± SEM of four or five animals from each condition studied.

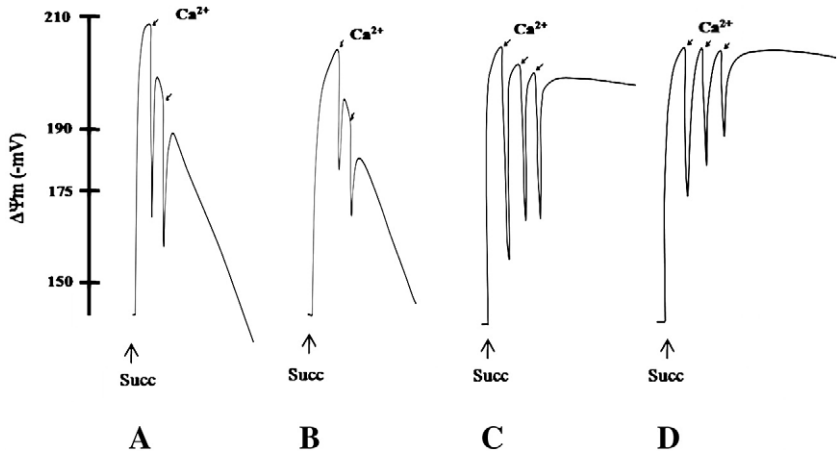

Fig. 2. Effect of DOX treatment on the loss of the mitochondrial transmembrane potential that characterizes the Ca^{2+}-induced permeability transition pore. Freshly isolated brain mitochondria (0.8 mg) in 1 ml of the reaction medium supplemented with 3 μl TPP^{+}were energized with 5 mM succinate. 0.85 μM CsA or 0.2 μg/ml oligomycin plus 100 μM ADP was added 1.5 min before mitochondrial energization. The traces are typical of six experiments. Trace A, saline-treated mitochondria; trace B, DOX-treated mitochondria; trace C, saline-treated mitochondria in the presence of oligomycin plus ADP; trace D, DOX-treated mitochondria in the presence of oligomycin plus ADP. Ca^{2+}pulses: first pulse 25 nmol Ca^{2+}, second and third pulses 20 nmol Ca^{2+}.

fluxes were measured, mitochondria isolated from DOX-treated animals and incubated with 45 nmol Ca^{2+}accumulated and retained less $Ca^{2+}$from the medium compared with control mitochondria (Fig. 3, traces A and B). However, the specific inhibitors of PTP, CsA (Fig. 3, traces C and D) and oligomycin plus ADP (Fig. 3, traces E and F), significantly increased the capacity of mitochondria to accumulate Ca^{2+}. In addition to $\Delta\Psi_m$ drop and Ca^{2+}overload, PTP induction also involves the oxidation of protein thiol groups. However, we did not observe significant differences in thiol groups of mitochondria from DOX-treated compared to saline-treated animals (data not shown).

Doxorubicin potentiates oxidative stress and damage

Mitochondrial aconitase activity is a sensitive redox sensor of reactive oxygen and nitrogen species in cells. As shown in Fig. 4, brain mitochondria isolated from DOX-treated rats presented a significantly lower aconitase activity compared with control mitochondria.

Lipid peroxidation is one particular marker of oxidative damage. To quantify the extent of lipid peroxidation the levels of TBARS and MDA were measured. As shown in Fig. 5A, in the absence of the pro-oxidant pair ADP/Fe^{2+}, the levels of TBARS were similar in both groups of experimental animals. However, the presence of ADP/Fe^{2+}induced a significant increase in the formation of TBARS in brain mitochondria isolated from the DOX-treated group compared with control mitochondria. Concerning MDA levels, no significant changes were observed between the two groups of experimental animals studied (Fig. 5B).

Doxorubicin alters the levels of mitochondrial antioxidants

Glutathione and vitamin E are important intracellular antioxidants, acting as free radical scavengers and, consequently, protecting cells against oxidative damage. Brain mitochondria isolated from the DOX-treated group presented a significant reduction in GSH levels compared with controls (Fig. 6A). Interestingly, DOX treatment

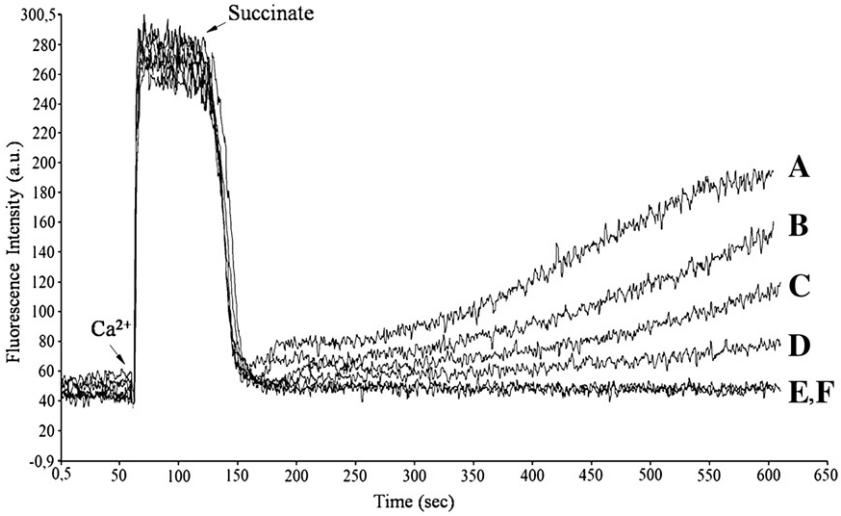

Fig. 3. Effect of DOX treatment on Ca^{2+} fluxes of brain mitochondria. Freshly isolated brain mitochondria (0.8 mg) in 2 ml of the reaction medium were energized with 5 mM succinate. Ca^{2+} (45 nmol) was added 1 min after mitochondria energization. CsA (0.85 μM) or oligomycin (0.2 μg/ml) plus ADP (100 μM) was added 2 min before Ca^{2+} addition. The traces are typical of six experiments. Trace A, DOX-treated mitochondria; trace B, saline-treated mitochondria; trace C, DOX-treated mitochondria in the presence of CsA; trace D, saline-treated mitochondria in the presence of CsA; trace E, DOX-treated mitochondria in the presence of oligomycin plus ADP; trace F, saline-treated mitochondria in the presence of oligomycin plus ADP.

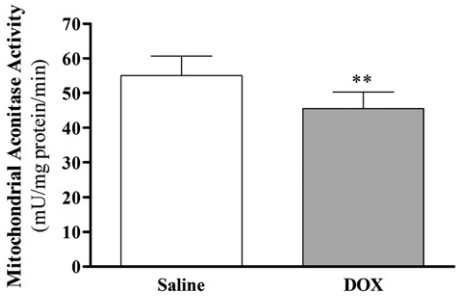

Fig. 4. Effect of DOX treatment on mitochondrial aconitase activity. Aconitase activity was measured as described under Materials and methods. Data shown represent means±SEM from four independent experiments. Statistical significance: $^{**}p < 0.01$ compared with control brain mitochondria.

induced a significant increase in vitamin E levels compared with control rats (Fig. 6B).

Discussion

The present study shows that although in vivo DOX does not affect the brain mitochondrial respiratory chain and phosphorylation system, it increases brain mitochondrial susceptibility to Ca^{2+}-induced PTP opening and oxidative damage. Indeed, it was observed that DOX treatment decreases the levels of GSH, mitochondrial aconitase activity, and the capacity of mitochondria to accumulate $Ca^{2+}$and increases TBARS levels. Interestingly, DOX treatment increases the levels of vitamin E that can represent a compensatory mechanism to fight oxidative damage.

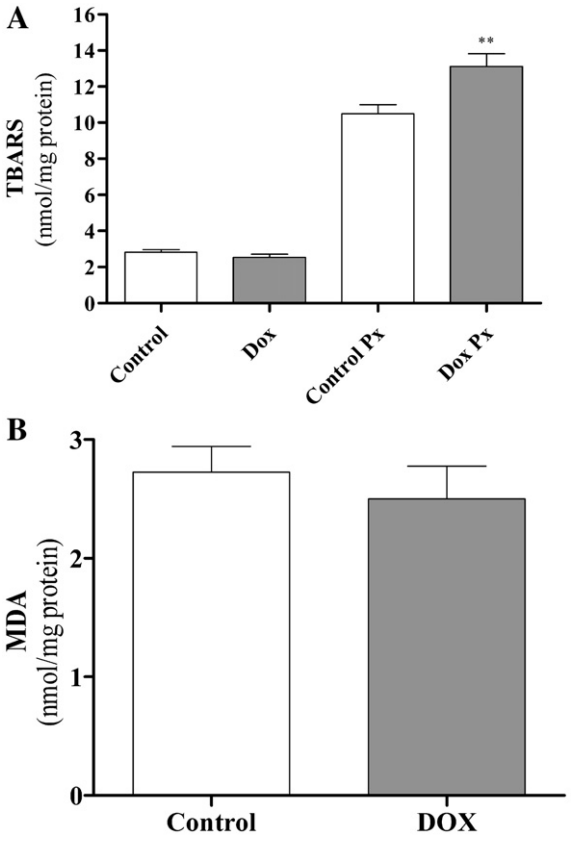

Fig. 5. Effect of DOX treatment on lipid peroxidation. (A) TBARS formation induced by the pro-oxidant pair ADP/$Fe^{2+}$and (B) MDA levels. Freshly isolated brain mitochondria were incubated at 1 mg/ml under standard conditions as described under Materials and methods. Data shown represent means±SEM from six to eight independent experiments. Statistical significance: $^{**}p<0.01$ compared with control brain mitochondria in the presence of ADP/Fe^{2+}.

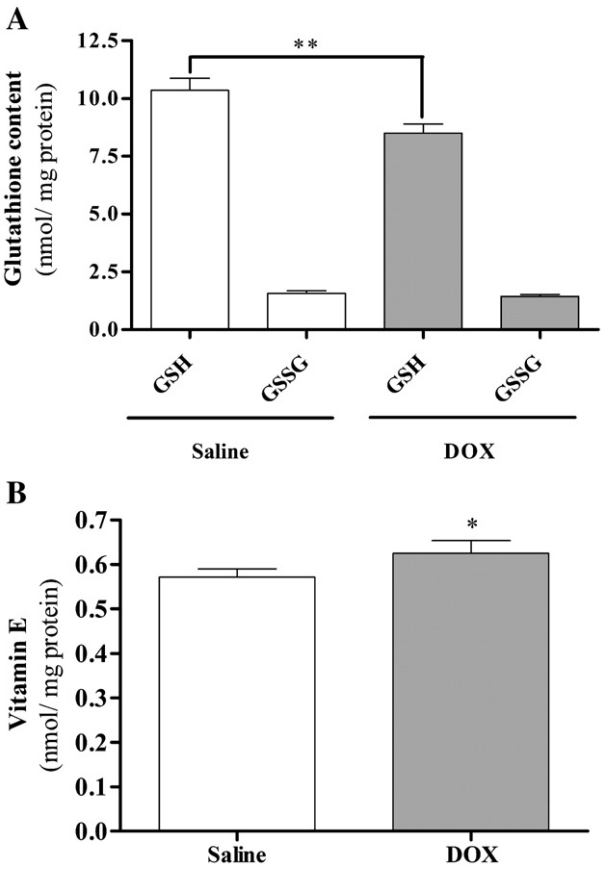

Fig. 6. Effect of DOX treatment on nonenzymatic antioxidant defenses. (A) Reduced (GSH) and oxidized (GSSG) glutathione and (B) vitamin E levels. Data shown represent means±SEM from six to eight independent experiments. Statistical significance: $^{**}p<0.01$; $^{*}p<0.05$ compared with control brain mitochondria.

Mitochondrial dysfunction promoted by DOX has been extensively studied in heart tissue [28–33] because cardiomyopathy is the most prominent side effect observed in patients that receive DOX therapy. However, much less is known about the effects of DOX treatment in the brain. Although previous studies indicate that cancer patients under DOX therapy present signs of cognitive decline [4], the mechanisms underlying these cognitive alterations remain unknown.

Because mitochondria seem to be a main target of DOX, we analyzed the effects of a subchronic administration of this antineoplastic agent on brain mitochondrial status. Our results show that DOX treatment does not induce significant alterations in States 2, 3, and 4 of mitochondrial respiration (Table 1); RCR; ADP/O index; oligomycin-inhibited respiration; or FCCP-stimulated respiration (Fig. 1). However, previous studies performed with heart [28,30,32] and brain [10,12,28] mitochondria show that DOX promotes an impairment of mitochondrial function. These discrepancies could be due to the experimental design or protocol used in each study and/or tissue-specific differences. Indeed, Tokarska-Schlattner and colleagues [28] evaluated the in vitro effect of DOX on heart and brain mitochondria and the authors observed that both types of mitochondria are affected by DOX. However, the results concerning brain mitochondria probably do not occur in vivo because DOX does not cross the blood–brain barrier [12]. Arnold and colleagues [34] performed liquid chromatography/electron-spray tandem mass spectroscopy to detect DOX and its metabolites in rat plasma and tissues. The authors reported that only one DOX metabolite (DOX-olone) can be detected in the brain

[34]. Interestingly, the same study shows that DOX-olone is not found in heart tissue [34], which may explain the differences promoted by DOX treatment on heart and brain tissue. Tangpong et al. [12] reported that DOX-induced brain mitochondrial impairment results from the increase in the circulating levels of TNF-α promoted by the administration of the drug. More recently, the same group also observed that DOX treatment promotes the impairment of the respiratory chain in brain mitochondria isolated from wild-type mice but not in those isolated from inducible nitric oxide synthase knockout mice, suggesting that in addition to TNF-α, nitric oxide also has a role in DOX-induced brain mitochondrial dysfunction [10]. However, we must note that the studies by Tangpong and collaborators [10,12] report the effect of a single injection of DOX (acute response), whereas the present work shows the effects of a subchronic administration of DOX. As previously discussed, the differences between the experimental designs probably result in the different effects observed. Indeed, we observed that seven weekly injections of DOX do not alter the respiratory chain, phosphorylation system, or energy levels (Fig. 1, Tables 1 and 2), which may indicate an adaptive response of brain mitochondria to chronic DOX treatment or that the oxidative phosphorylation apparatus is not affected by DOX.

Mitochondrial Ca^{2+}loading capacity is a measure of the total amount of Ca^{2+}that mitochondria are able to accumulate from the incubation medium before undergoing the PTP leading to Ca^{2+}release back to the medium [35]. There are several studies reporting that DOX causes a decrease in the capacity of isolated cardiac mitochondria to accumulate and retain Ca^{2+}[35–38]. Accordingly, we observed that DOX-treated mitochondria present a lower Ca^{2+}retention capacity compared with saline-treated mitochondria (Fig. 3, traces A and B). Previously, Zhou et al. [35] showed that the decrease in Ca^{2+}loading capacity promoted by DOX treatment is not reversed over a 5-week period after the discontinuation of the treatment, suggesting that the alteration of mitochondrial Ca^{2+}regulation induced by DOX is persistent and irreversible. In accordance with previous studies, preincubation of mitochondria with oligomycin plus ADP or CsA, the inhibitors of PTP, significantly increased the capacity of mitochondria to accumulate Ca^{2+}[6,39–41]. It is known that the PTP is potentiated upon the oxidation of protein thiol groups in the pore complex [42]. However, we did not observe any significant difference in the levels of oxidized thiols (data not shown). Zhou et al. [35] suggested that the oxidative alteration of mitochondrial proteins is not a major factor responsible for the decrease in mitochondrial Ca^{2+}retention caused by DOX. However, a previous study from our laboratory [43] shows that thiol-dependent alteration of PTP is an important factor in DOX-induced cardiac mitochondrial dysfunction. As previously discussed, these results may reflect tissue-specific differences.

Growing evidence suggests that cognitive decline and neurodegenerative disorders are associated with high levels of oxidative stress [44]. Free radical-mediated oxidative stress has been proposed as a potential mechanism underlying DOX toxicity in the brain [4]. In accordance, we observed that DOX treatment increases TBARS levels (Fig. 5A). Previous studies show that DOX treatment promotes lipid peroxidation in brain, heart, liver, lung, and kidney tissues [45–47]. Furthermore, Oz and Ilhan [47] reported that DOX-treated rats undergoing cotreatment with melatonin, a free radical scavenger and antioxidant compound, presented lower levels of lipid peroxidation in kidney, lung, liver, and brain.

GSH, a crucial nonenzymatic antioxidant defense, has a pivotal role in the maintenance of cells' redox state. GSH is a cofactor of several detoxifying enzymes and is able to regenerate important antioxidants, such as vitamin E [48]. Recently, it has been shown that the brains of DOX-treated mice presented lower GSH levels compared with control animals [49]. In accordance, we also observed a significant decrease in GSH levels in brain mitochondria isolated from DOX-treated animals (Fig. 6A). However, we also observed a significant increase in vitamin E levels induced by DOX treatment (Fig. 6B). The increase in vitamin E levels (Fig. 6B) could represent a compensatory mechanism to counteract the increase in lipid peroxidation (Fig. 5A) promoted by DOX treatment. The decrease in GSH levels could also be related with the increased levels of vitamin E observed in DOX-treated mitochondria (Fig. 6) because GSH is involved in vitamin E regeneration [48].

Another important marker of oxidative damage is the loss of the mitochondrial aconitase activity, the inactivity of this enzyme being an indicator of superoxide ($O_2^{\cdot-}$) generation in mitochondria [50,51]. Mitochondrial aconitase contains a $[4Fe–4S]^{2+}$cluster in its active site, which is oxidized by $O_2^{\cdot-}$ and related species, generating the inactive $[3Fe–4S]^{1+}$aconitase [52]. Moreover, $O_2^{\cdot-}$-mediated mitochondrial aconitase inactivation leads to hydroxyl radical formation [53]. Minotti and collaborators [54] reported that doxorubicinol, the secondary alcohol metabolite of doxorubicin, irreversibly inactivates aconitase, contributing to DOX-induced cardiotoxicity. We also observed that DOX treatment induces a significant decrease in brain mitochondrial aconitase activity (Fig. 4), which reinforces the idea that animals subjected to DOX treatment present high levels of oxidative stress. Recently, it has been shown that heat shock protein 27 protects the aconitase activity of cardiac cells by increasing the activity of superoxide dismutase [55].

Is important to note that although DOX treatment did not induce significant alterations in the respiratory parameters (Table 1 and Fig. 1), it induced a significant decrease in aconitase activity (Fig. 4) and increase in the susceptibility to Ca^{2+}-induced PTP (Figs. 2, trace B, and 3, trace A), suggesting that the standard respiratory assays (RCR and ADP/O index) may not be sufficiently sensitive to detect mitochondrial alterations caused by subchronic treatments.

In summary, our results show that DOX treatment increases the susceptibility of mitochondria to oxidative stress and Ca^{2+}-induced PTP opening, which may predispose to cognitive impairment and development of neurodegenerative conditions. Nevertheless, future studies are needed to correlate oxidative mitochondrial alterations induced by DOX with neurodegenerative conditions. Also, the present study highlights the need to develop antioxidant strategies to counteract DOX-induced brain mitochondrial oxidative stress.

Acknowledgment

The work was funded by the Portuguese Foundation for Science and Technology (PTDC-SAU-OSM-64084-2006).

References

[1] Wallace, K. B. Adriamycin-induced interference with cardiac mitochondrial calcium homeostasis. *Cardiovasc. Toxicol.* **7:**101–107; 2007.
[2] Lopes, M. A.; Meisel, A.; Dirnagl, U.; Carvalho, F. D.; Bastos, M. L. Doxorubicin induces biphasic neurotoxicity to rat cortical neurons. *NeuroToxicology* **29:**286–293; 2008.
[3] Berthiaume, J. M.; Wallace, K. B. Adriamycin-induced oxidative mitochondrial cardiotoxicity. *Cell Biol. Toxicol.* **23:**15–25; 2007.
[4] Chen, Y.; Jungsuwadee, P.; Vore, M.; Butterfield, D. A.; St. Clair, D. K. Collateral damage in cancer chemotherapy: oxidative stress in nontargeted tissues. *Mol. Interv.* **7:**147–156; 2007.
[5] Butterfield, D. A.; Lauderback, C. M. Lipid peroxidation and protein oxidation in Alzheimer's disease brain: potential causes and consequences involving amyloid -peptide-associated free radical oxidative stress. *Free Radic. Biol. Med.* **32:**1050–1060; 2002.
[6] Moreira, P. I.; Smith, M. A.; Zhu, X.; Nunomura, A.; Castellani, R. J.; Perry, G. Oxidative stress and neurodegeneration. *Ann. N. Y. Acad. Sci.* **1043:**545–552; 2005.
[7] Park, E. S.; Kim, S. D.; Lee, M. H.; Lee, H. S.; Lee, I. S.; Sung, J. K.; Yoon, Y. S. Protective effects of N-acetylcysteine and selenium against doxorubicin toxicity in rats. *J. Vet. Sci.* **4:**129–136; 2003.
[8] Duchen, M. R. Roles of mitochondria in health and disease. *Diabetes* **53:**96–102; 2004.
[9] Starkov, A. A.; Wallace, K. B. Structural determinants of fluorochemical-induced mitochondrial dysfunction. *Toxicol. Sci.* **66:**244–252; 2002.
[10] Tangpong, J.; Cole, M. P.; Sultana, R.; Estus, S.; Vore, M.; St. Clair, W.; Ratanachaiyavong, S.; St. Clair, D. K.; Butterfield, D. A. Adriamycin-mediated nitration of manganese superoxide dismutase in the central nervous system: insight into the mechanism of chemobrain. *J. Neurochem.* **100:**191–201; 2007.

[11] Yen, H. C.; Oberley, T. D.; Vichitbandha, S.; Ho, Y. S.; St. Clair, D. K. The protective role of manganese superoxide dismutase against adriamycin-induced acute cardiac toxicity in transgenic mice. *J. Clin. Invest.* **98:**1253–1260; 1996.

[12] Tangpong, J.; Cole, M. P.; Sultana, R.; Joshi, G.; Estus, S.; Vore, M.; St. Clair, W.; Ratanachaiyavong, S.; St. Clair, D. K.; Butterfield, D. A. Adriamycin-induced TNF-α-mediated central nervous system toxicity. *Neurobiol. Dis.* **23:**127–139; 2006.

[13] Chaiswing, L.; Cole, M. P.; Ittarat, W.; Szweda, L. I.; St. Clair, D. K.; Oberley, T. D. Manganese superoxide dismutase and inducible nitric oxide synthase modify early oxidative events in acute adriamycin-induced mitochondrial toxicity. *Mol. Cancer Ther.* **4:**1056–1064; 2005.

[14] Rosenthal, R. E.; Hamud, F.; Fiskum, G.; Varghese, P. J.; Sharpe, S. Cerebral ischemia and reperfusion: prevention of brain mitochondrial injury by lidoflazine. *J. Cereb. Blood Flow Metab.* **7:**752–758; 1987.

[15] Gornall, A. G.; Bardawill, C. J.; David, M. M. Determination of serum proteins by means of the biuret reaction. *J. Biol. Chem.* **177:**751–766; 1949.

[16] Estabrook, R. E. Mitochondrial respiratory control and the polarographic measurement of ADP/O ratios. *Methods Enzymol.* **10:**41–47; 1967.

[17] Kamo, N.; Muratsugu, M.; Hongoh, R.; Kobatake, Y. Membrane potential of mitochondria measured with an electrode sensitive to tetraphenylphosphonium and relationship between proton electrochemical potential and phosphorylation potential in steady state. *J. Membr. Biol.* **49:**105–121; 1979.

[18] Jensen, B. D.; Gunter, T. R. The use of tertaphenylphosphonium (TPP^+) to measure membrane potentials in mitochondria: membrane binding and respiratory effects. *Biophys. J.* **45:**92; 1984.

[19] Muratsugu, M.; Kamo, N.; Kurihara, K.; Kobatake, Y. Selective electrode for dibenzyl dimethyl ammonium cation as indicator of the membrane potential in biological systems. *Biochim. Biophys. Acta* **464:**613–619; 1977.

[20] Rajdev, S.; Reynolds, I. J. Calcium green-5N, a novel fluorescent probe for monitoring high intracellular free Ca^{2+} concentrations associated with glutamate excitotoxicity in cultured rat brain neurons. *Neurosci. Lett.* **162:**149–152; 1993.

[21] Riddles, P. W.; Blakeley, R. L.; Zerner, B. Reassessment of Ellman's reagent. *Methods Enzymol.* **91:**49–60; 1983.

[22] Ernster, L.; Nordenbrand, K. Microsomal lipid peroxidation. *Methods Enzymol.* **10:**574–580; 1967.

[23] Wong, S. H.; Knight, J. A.; Hopfer, S. M.; Zaharia, O.; Leach Jr., C. N.; Sunderman Jr., F. W. Lipoperoxides in plasma as measured by liquid-chromatographic separation of malondialdehyde–thiobarbituric acid adduct. *Clin. Chem.* **33:**214–220; 1987.

[24] Hissin, P. J.; Hilf, R. A fluorometric method for determination of oxidized and reduced glutathione in tissues. *Anal. Biochem.* **74:**214–226; 1976.

[25] Vatassery, G. T.; Younoszai, R. Alpha tocopherol levels in various regions of the central nervous systems of the rat and guinea pig. *Lipids* **13:**828–831; 1978.

[26] Krebs, H. A.; Holzach, O. The conversion of citrate into cis-aconitate and isocitrate in the presence of aconitase. *Biochem. J.* **52:**527–528; 1952.

[27] Tsujimoto, Y.; Shimizu, S. A role of the mitochondrial membrane permeability transition in cell death. *Apoptosis* **12:**835–840; 2007.

[28] Tokarska-Schlattner, M.; Dolder, M.; Gerber, I.; Speer, O.; Wallimann, T.; Schlattner, U. Reduced creatine-stimulated respiration in doxorubicin challenged mitochondria: particular sensitivity of the heart. *Biochim. Biophys. Acta* **1767:**1276–1284; 2007.

[29] Daosukho, C.; Chen, Y.; Noel, T.; Sompol, P.; Nithipongvanitch, R.; Velez, J. M.; Oberley, T. P.; St. Clair, D. K. Phenylbutyrate, a histone deacetylase inhibitor, protects against adriamycin-induced cardiac injury. *Free Radic. Biol. Med.* **42:**1818–1825; 2007.

[30] Lebrecht, D.; Setzer, B.; Ketelsen, U. P.; Haberstroh, J.; Walker, U. A. Time-dependent and tissue-specific accumulation of mtDNA and respiratory chain defects in chronic doxorubicin cardiomyopathy. *Circulation* **108:**2423–2429; 2003.

[31] Muhammed, H.; Kurup, C. K. R. Influence of ubiquinone on the inhibitory effect of adriamycin on mitochondrial oxidative phosphorylation. *Biochem. J.* **217:**493–498; 1984.

[32] Clementi, M. E.; Giardina, B.; Di Stasio, E.; Mordente, A.; Misiti, F. Doxorubicin-derived metabolites induced release of cytochrome c and inhibition of respiration on cardiac isolated mitochondria. *Anticancer Res.* **23:**2445–2450; 2003.

[33] Oliveira, P. J.; Bjork, J. A.; Santos, M. S.; Leino, R. L.; Froberg, M. K.; Moreno, A. J.; Wallace, K. B. Carvedilol-mediated antioxidant protection against doxorubicin-induced cardiac mitochondrial toxicity. *Toxicol. Appl. Pharmacol.* **200:**159–168; 2004.

[34] Arnold, R. D.; Slack, J. E.; Straubinger, R. M. Quantification of doxorubicin and metabolites in rat plasma and small volume tissue samples by liquid chromatography/electrospray tandem mass spectroscopy. *J. Chromatogr. B* **808:**141–152; 2004.

[35] Zhou, S.; Starkov, A.; Froberg, M. K.; Leino, R. L.; Wallace, K. B. Cumulative and irreversible cardiac mitochondrial dysfunction induced by doxorubicin. *Cancer Res.* **61:**771–777; 2001.

[36] Santos, D. L.; Moreno, A. J.; Leino, R. L.; Froberg, M. K.; Wallace, K. B. Carvedilol protects against doxorubicin-induced mitochondrial cardiomyopathy. *Toxicol. Appl. Pharmacol.* **185:**218–227; 2002.

[37] Solem, L. E.; Heller, L. J.; Wallace, K. B. Dose-dependent increase in sensitivity to calcium-induced mitochondrial dysfunction and cardiomyocyte cell injury by doxorubicin. *J. Mol. Cell. Cardiol.* **28:**1023–1032; 1996.

[38] Singal, P. K.; Forbes, M. S.; Sperelakis, N. Occurrence of intramitochondrial Ca^{2+} granules in a hypertrophied heart exposed to adriamycin. *Can. J. Physiol. Pharmacol.* **62:**1239–1244; 1984.

[39] Maciel, E. N.; Vercesi, A. E.; Castilho, R. F. Oxidative stress in Ca^{2+}-induced membrane permeability transition in brain mitochondria. *J. Neurochem.* **79:**1237–1245; 2001.

[40] Brustovetsky, N.; Dubinsky, J. M. Limitations of cyclosporin A inhibition of the permeability transition in CNS mitochondria. *J. Neurosci.* **20:**8229–8237; 2000.

[41] Moreira, P. I.; Custdio, J. B.; Oliveira, C. R.; Santos, M. S. Hydroxytamoxifen protects against oxidative stress in brain mitochondria. *Biochem. Pharmacol.* **68:**195–204; 2004.

[42] Kowaltowski, A. J.; Castilho, R. F.; Vercesi, A. E. Mitochondrial permeability transition and oxidative stress. *FEBS Lett.* **495:**12–15; 2001.

[43] Oliveira, P. J.; Santos, M. S.; Wallace, K. B. Doxorubicin-induced thiol-dependent alteration of cardiac mitochondrial permeability transition and respiration. *Biochemistry (Moscow)* **71:**194–199; 2006.

[44] Drge, W.; Schipper, H. M. Oxidative stress and aberrant signaling in aging and cognitive decline. *Aging Cell* **6:**361–370; 2007.

[45] Julka, D.; Sandhir, R.; Gill, K. D. Adriamycin-induced oxidative stress in rat central nervous system. *Biochem. Mol. Biol. Int.* **29:**807–820; 1993.

[46] Agapito, M. T.; Antoln, Y.; del Brio, M. T.; Lpez-Burillo, S.; Pablos, M. I.; Recio, J. M. Protective effect of melatonin against adriamycin toxicity in the rat. *J. Pineal Res.* **31:**23–30; 2001.

[47] Oz, E.; Ilhan, M. N. Effects of melatonin in reducing the toxic effects of doxorubicin. *Mol. Cell Biochem.* **286:**11–15; 2006.

[48] Valko, M.; Leibfritz, D.; Moncol, J.; Cronin, M. T.; Mazur, M.; Telser, J. Free radicals and antioxidants in normal physiological functions and human disease. *Int. J. Biochem. Cell Biol.* **39:**44–84; 2007.

[49] Joshi, G.; Hardas, S.; Sultana, R.; St Clair, D. K.; Vore, M.; Butterfield, D. A. Glutathione elevation by -glutamyl cysteine ethyl ester as a potential therapeutic strategy for preventing oxidative stress in brain mediated by in vivo administration of adriamycin: implication for chemobrain. *J. Neurosci. Res.* **85:**497–503; 2007.

[50] Li, Q. Y.; Pedersen, C.; Day, B. J.; Patel, M. Dependence of excitotoxic neurodegeneration on mitochondrial aconitase inactivation. *J. Neurochem.* **78:**746–755; 2001.

[51] Sipos, I.; Tretter, L.; Adam-Vizi, V. Quantitative relationship between inhibition of respiratory complexes and formation of reactive oxygen species in isolated nerve terminals. *J. Neurochem.* **84:**112–118; 2003.

[52] Vasquez-Vivar, J.; Kalyanaraman, B.; Kennedy, M. C. Mitochondrial aconitase is a source of hydroxyl radical: an electron spin resonance investigation. *J. Biol. Chem.* **275:**14064–14069; 2000.

[53] Flint, D. H.; Tuminello, J. F.; Emptage, M. H. The inactivation of Fe–S cluster containing hydrolyases by superoxide. *J. Biol. Chem.* **268:**22369–22376; 1993.

[54] Minotti, G.; Recalcati, S.; Mordente, A.; Liberi, G.; Calafiore, A. M.; Mancuso, C.; Preziosi, P.; Cairo, G. The secondary alcohol metabolite of doxorubicin irreversibly inactivates aconitase/iron regulatory protein-1 in cytosolic fractions from human myocardium. *FASEB J.* **12:**541–552; 1998.

[55] Turakhia, S.; Venkatakrishnan, C. D.; Dunsmore, K.; Wong, H.; Kuppusamy, P.; Zweier, J. L.; Ilangovan, G. Doxorubicin-induced cardiotoxicity: direct correlation of cardiac fibroblast and H9c2 cell survival and aconitase activity with heat shock protein 27. *Am. J. Physiol. Heart Circ. Physiol* . **293:**H3111–H3121; 2007.